IMPEDANCE CURE AND FLOW MONITORING IN THE PROCESSING OF ADVANCED COMPOSITES

Alexandros A Skordos* and Ivana K Partridge*

ABSTRACT

The paper presents recent developments in the area of impedance cure and flow monitoring of thermosetting matrix/continuous reinforcement composites. Impedance cure monitoring is a variation of dielectric cure monitoring which follows the progress of the curing reaction and the accompanying structural phenomena by means of the impedance spectrum response of the curing material. Currently, a good correlation between specific features of the imaginary impedance spectrum and the progress of the reaction has been found to hold under isothermal conditions. In this paper the correlation between the impedance and the progress of the reaction is extended to dynamic cure conditions. Impedance flow monitoring of the filling stage of liquid moulding of glass composites, based on lineal sensors, has been developed and reported recently. Here, this technique is extended to the case of conductive reinforcements with the development of a new sensing system. The system performance is tested against visual observation of the flow front position during resin transfer moulding.

INTRODUCTION

In recent years the need for predictive modelling and for in-situ real time monitoring of composites manufacturing processes has arisen and been met by the development of a family of appropriate techniques. The modelling of the cure stage of composites manufacturing has been investigated extensively [1-6] and cure monitoring methods, such as dielectric [7,8], fibre optic [9,10] and acoustic cure monitoring [11-12], begun to be implemented in an industrial environment. Very recently an interest in flow monitoring techniques based on optical fibre, dc conductivity and dielectric measurements and appropriate for the measurement of filling progress during liquid composite moulding started to be developed [13-16].

Dielectric cure monitoring techniques are based on the dependence of the electric and dielectric measures (complex dielectric constant, conductivity and impedance) on structural properties of the curing system (degree of cure, glass transition temperature and viscosity). The behaviour of a thermoset, when an AC electric field is applied to it, is governed by three phenomena: (i) dipole polarisation, (ii) migrating charges conduction and (iii) electrode polarisation.

A few research groups have chosen to present and process dielectric cure monitoring results in terms of the complex impedance. The essential meaning of the measurement is exactly the same as in the dielectric constants representation, as the phenomena taking place are identical, but in some cases the impedance representation appears to be more natural. In impedance monitoring the electric response of a thermosetting system can be represented by an equivalent circuit, the most widely used circuit is illustrated in Fig. 1 [17-19]. The presence of dipolar relaxation is accounted for by introducing a capacitor C_{sd}, in series with a resistor R_{sd}, corresponding to the permanent dipoles and connected in parallel with another

* Advanced Materials Department, Cranfield University, Bedford, MK43 0AL, UK

capacitance C_{id}, corresponding to the induced dipoles. The migrating charges mechanism is represented by a resistor R_I connected in parallel with the dipolar relaxation sub-circuit and the electrode polarisation by two capacitors C_e, one for each electrode, connected in series with the overall circuit. The complex impedance of the circuit is [19]:

$$Z = Z' - jZ'' \qquad [1]$$

where

$$Z' = \frac{R_i\left[\omega^2 C_{sd}{}^2 R_{sd}\left(R_{sd}+R_i\right)+1\right]}{\omega^2\left(C_{sd}R_i + C_{sd}R_{sd} + C_{id}R_i\right)^2 + \left(\omega^2 C_{sd}R_{sd}R_i C_{id} - 1\right)^2} \qquad [2]$$

$$Z'' = \frac{R_i\left[\omega^3 C_{sd}{}^2 R_{sd}{}^2 R_i C_{id} + \omega R_i\left(C_{id}+C_{sd}\right)\right]}{\omega^2\left(C_{sd}R_i + C_{sd}R_{sd} + C_{id}R_i\right)^2 + \left(\omega^2 C_{sd}R_{sd}R_i C_{id} - 1\right)^2} + \frac{2}{C_e\omega} \qquad [3]$$

The impedance spectrum of such a circuit is illustrated in Fig. 2. The response at low frequencies is dominated by the electrode polarisation effect, the conduction mechanism becomes dominant at intermediate frequencies and the dipolar relaxation at high frequencies.

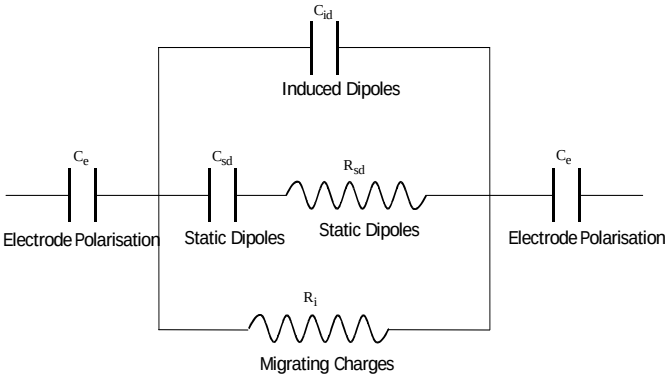

Fig. 1 *Equivalent circuit representation of the electrical response of thermosetting materials*

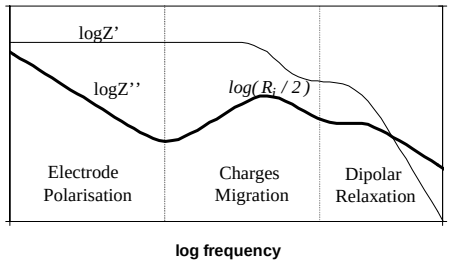

Fig. 2 *Impedance spectrum of the electrode polarisation-charge migration-dipolar relaxation circuit*

The application of monitoring to industrial situations requires the translation of the impedance results to information related to the chemical or the structural state of the curing material. A correlation between the progress of the reaction and the logarithm of the resistivity as estimated using the peak imaginary impedance value (Fig. 2) has been established. The correlation between normalised resistivity and fractional conversion under isothermal conditions can be expressed as [18, 19]:

$$\alpha = \alpha_{max}\frac{log\,\tilde{\rho} - log\,\tilde{\rho}_o}{log\,\tilde{\rho}_{max} - log\,\tilde{\rho}_o} \qquad [4]$$

where α_{max} is the maximum degree of cure at the curing temperature, $\tilde{\rho}$ the resistivity, $\tilde{\rho}_o$ the resistivity of the unreacted resin and $\tilde{\rho}_{max}$ the resistivity of the fully reacted resin.

Empirical evidence suggests that some of the structural phenomena taking place during the cure are manifested in impedance signal. More specifically, vitrification has been found to coincide with a knee in the imaginary impedance versus time curve and a peak in the real impedance versus time curve [19, 20], but the underlying molecular mechanisms causing this correlation have not been elucidated.

Impedance flow monitoring is based on the significant differences between the electric properties of dry and wetted areas of a composite pre-form. A lineal sensor with a semi-cylindrical fringing field placed along the flow path of a non-conductive reinforcement can monitor the progress of filling as it is covered gradually by resin. A sensing setup

implementing this principle has been applied successfully to the filing of glass reinforced preforms [16]. In that case the covered length of the sensor is a linear function of the complex admittance as follows]16]:

$$l_w = \frac{Y_{sensor} - Y_{dry}}{Y_{cov} - Y_{dry}} l_t \qquad [5]$$

where Y_{dry} is the admittance of the dry sensor and Y_{cov} is the admittance measured when the sensor is fully covered.

In this study results leading to the extension of the applicability of impedance monitoring in composites processing are presented. The impedance cure monitoring response of an epoxy resin is investigated under isothermal and dynamic curing conditions and a methodology correlating impedance signals with fractional conversion under both dynamic and isothermal conditions is established. Impedance flow monitoring is extended to conductive reinforcement with the design implementation and validation of a new sensing setup appropriate for carbon pre-forms.

EXPERIMENTAL DETAILS

A. Cure monitoring

An epoxy resin appropriate for resin transfer moulding (Hexcel, RTM6) has been used in this study. Impedance cure monitoring measurements were performed using a Solartron SI 1260 frequency response analyser. The instrument communicated with a computer via an IEEE interface. A purpose built software code has been utilised to drive the frequency response analyser and collect the raw data. Commercial sensors (GIA) comprising an assembly of interdigitated electrodes printed on a polymeric film were used in this study. After soldering on the cables that connect the analyser to the sensor, the sensor was immersed in a glass tube containing liquid resin. Then the glass tube was placed in a hollow copper cylinder surrounded by heating elements, which were controlled by a Eurotherm temperature controller. A control thermocouple was placed in a hole on the wall of the hollow cylinder. A second thermocouple was placed in the glass tube in order to record the actual thermal profile of the resin. Isothermal cure experiments on RTM6 epoxy resin were performed at 130, 140, 150 and 160 ^{o}C and dynamic cure experiments were performed at at 0.25, 0.5, 0.75, 1, 1.25, 1.5, 1.75 and 2 ^{o}C/min. The measurements were performed in the frequency range between 1 Hz and 1 MHz. Twenty-five frequencies were swept on a logarithmic scale.

B. Flow monitoring

The sensing setup comprises an array of thin insulated wires, that are in contact with the carbon preform and are connected to the impedance analyser. The reinforcement is connected to the analyser and the measurement is performed between the array of wires and the fibres of the pre-form. A schematic of the arrangement of fibre tows and wires is given in Fig. 3. In the case illustrated, the wires are in contact with the RTM glass tool. As the fibre tows conform around the hard wire some pores are formed. With the application of a voltage an electric field is formed between the conductive core of the wire and the fibre. The field occupies the insulating coating of the wire and the pore regions. When the reinforcement is dry the pores are filled with air. As the impregnation process progresses more and more of the pores are filled with the resin. Similarly to the glass reinforcement case, it is expected that the difference in electrical properties of air and of the liquid resin will result in gradual change in the electrical response as the filling progresses.

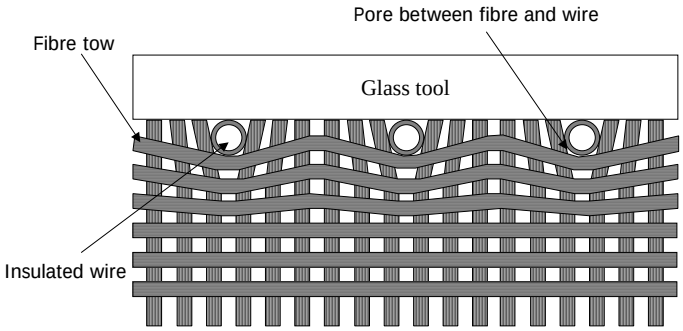

Fig. 3 *Sensing configuration for flow monitoring in carbon reinforcements*

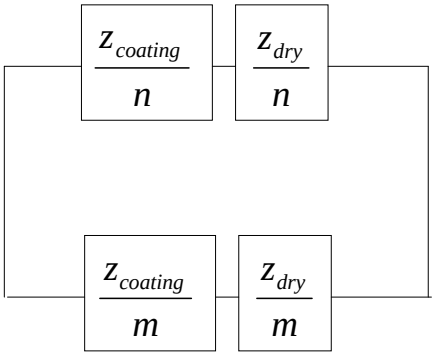

Fig. 4 *Equivalent circuit representing the response of the flow sensing setup*

The sensing configuration can be considered as the sum of a number of wire and fabric segments with length unity. Assuming that the carbon reinforcement is under uniform potential, all the segments corresponding to one wire are connected in parallel. Each of these segments contains two elements connected in series, one corresponding to the insulating coating and one to the pores. If the unit length is large compared with the size of the pores, the impedance of the element corresponding to pores will be equal to z_{dry} for all the n segments in the dry region of the mould, and equal to z_{wetted} for all the m segments in the wetted region. This situation can be represented by the circuit of Fig. 4. Consequently, the following equation is expected to hold:

$$Y_{sensor} = m\left(\frac{z_d - z_w}{z_c^2 + z_c z_d + z_c z_w + z_w z_d}\right) + \left(\frac{(m+n)z_c + (m+n)z_w}{z_c^2 + z_c z_d + z_c z_w + z_w z_d}\right) \quad [6]$$

where z_c denotes the impedance per unit length of the insulating layer of the sensing wire. Similarly to the case of the glass reinforcement, a linear expression of the sensor admittance as a function of the length of the wire in contact with liquid resin (Eq. 5) can be derived.

The sensor performance was validated during the filling and curing of a continuous carbon fibre/RTM6 composite in a partially transparent RTM tool. The carbon non-crimped fabric reinforcement (CTLX, BTI Europe) had a surface density of 816 g/m^2 and comprised three plies with +45/-45/0 orientations. Four layers of this fabric were used, making the total lay-up sequence $(+45/-45/0/0/-45/+45)_{2S}$. The fibre weight fraction in the laminate was 69%. The sensor comprised an array of three insulated (polyurethane coated) copper wires, with a diameter of 0.25 mm, placed in the centre of the mould in contact with the glass top tooling. The distance between the wires was 2 mm. The sensor length was 28 cm and the mould thickness 3.3 mm. The filling was performed at 120^{o}C. Visual determination of the flow front position was recorded against time. After completion of the filling stage the mould temperature was increased to 160^{o}C to cure the composite.

RESULTS

A. Cure monitoring

The evolution of real and imaginary impedance spectra during the cure at 150 ^{o}C is illustrated in Fig. 5. The results of isothermal experiments at 130,140 and 160 ^{o}C show equivalent behaviour. It can be observed that the real impedance spectrum comprises a plateau at low frequencies and a region where the impedance decreases as the frequency increases. The latter region starts as a linear decrease, which becomes less intense towards very high

frequencies, indicating the existence of another plateau at frequencies beyond 1 MHz. The imaginary impedance spectrum comprises three linear regions separated by a minimum and a maximum. At very low frequencies imaginary impedance decreases with frequency, reaches a minimum value and then increases up to a maximum. Further increase of the frequency results in a linear decrease of the imaginary impedance logarithm. Both spectra show a strong dependence upon material state as it changes during the cure. The real impedance plateau value increases as the curing progresses, whereas the frequency where the plateau ends decreases. Both the minimum and maximum of imaginary impedance increase as curing progresses. The whole imaginary impedance spectrum is shifted to lower frequencies as the reaction progresses but, unlike in the case of the real impedance the final linear part remains constant.

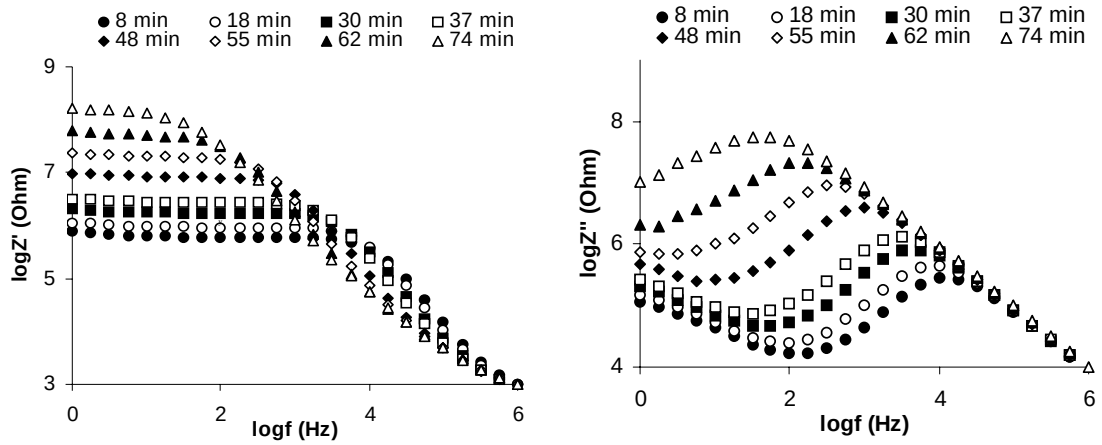

(a) Real impedance (b) Imaginary impedance

Fig.5 *Impedance spectra evolution during isothermal cure at 150 ^oC*

The evolution of the real and imaginary impedance spectra for the experiment at 0.25 ^oC/min is illustrated in Fig. 6. The behaviour illustrated in Fig. 6 is characteristic of all dynamic cure experiments of RTM6 epoxy resin. The form of both spectra is identical to the isothermal case, i.e. the real impedance spectrum comprises a plateau and a linear decrease region, and the imaginary impedance spectrum comprises a minimum, a maximum and three linear regions. However, the evolution of the spectra is more complicated in the dynamic case due to the combined influences of temperature and of state-of-material changes. In the initial stages of the dynamic cure the real impedance plateau value decreases and the frequency where the plateau ends increases (curves at 50 and 100 ^oC in Fig. 6a) as a result of the rise in temperature. At higher temperatures (curves at 135, 140 and 150 ^oC in Fig. 6a) the spectrum shows the behaviour observed in isothermal cure, i. e. the plateau value increases and the plateau end frequency decreases. This can be attributed to the domination of material state connected phenomena to the signal. When temperature increases further the situation reverses (curves at 170, 180, 190 and 210 ^oC in Fig. 6a) and due to temperature changes domination in the signal, the plateau value decreases and the plateau end frequency increases. Analogous phenomena are observed in the evolution of the imaginary impedance spectrum. At low temperatures the spectrum is shifted to higher frequencies and the maximum and minimum values decrease (curves at 50 and 100 ^oC in Fig. 6b). At intermediate temperatures (curves at 135, 140 and 150 ^oC in Fig. 6b) the behaviour observed in isothermal cure is reproduced, i.e. the spectrum is shifted to lower frequencies and the maximum and minimum values increase, implying material state changes domination. Further increase in temperature (curves at 170,

180, 190 and 210 ^{o}C in Fig. 6b) leads to temperature changes domination, i.e. the whole spectrum is shifted to higher frequencies and the maximum and minimum values decrease.

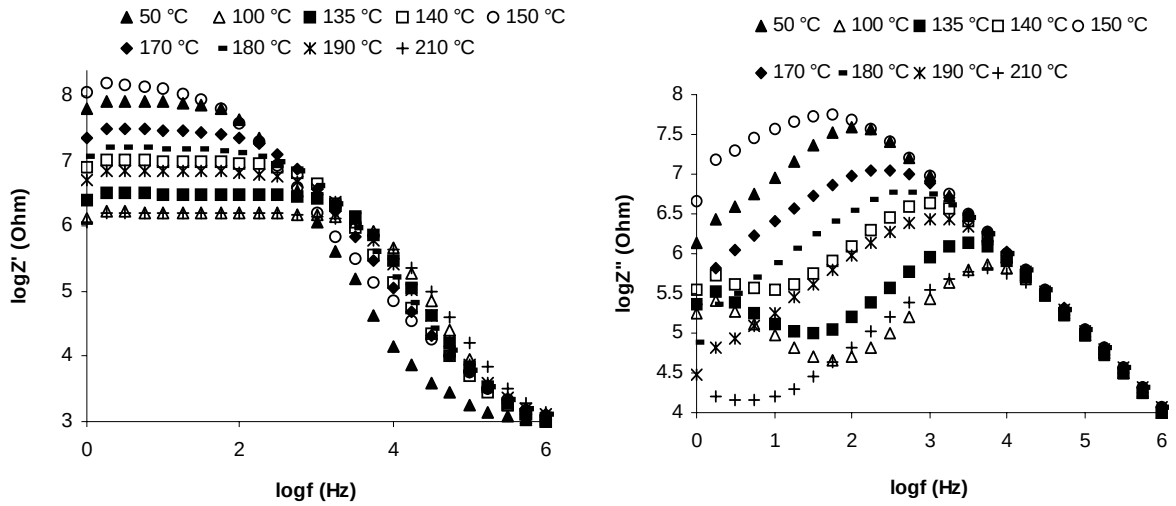

(a) Real impedance (b) Imaginary impedance

Fig.6 *I impedance spectrum evolution during dynamic cure at 0.25 ^{o}C/min*

It has been shown that following the changes of the imaginary impedance spectrum maximum can give an accurate estimation of the fractional conversion under isothermal conditions [18, 19]. In Figs. 7 and 8 the evolution of the imaginary impedance maximum together with the degree of cure evolution, as calculated using the kinetic model described elsewhere [21], for the isothermal experiments at 130, 140, 150 and 160 ^{o}C and the dynamic experiments at 0.25, 0.5, 0.75 are given. Lines indicating the cure time of maximum reaction rate in each experiment are superimposed on the curves, in order to facilitate the comparison between impedance and progress of reaction data. In Fig. 7 it can be observed that the imaginary impedance maximum imitates the conversion curves very closely. The start, end and maximum rate points are very similar in the two curves. Thus, normalisation of the impedance data can lead to a direct estimation of the reaction progress in isothermal experiments. In contrast, under dynamic conditions, as illustrated in Fig. 8, the combined influence of temperature and reaction complicates the imaginary impedance maximum behaviour. At the beginning of the curing temperature governs the maximum value, which drops as the viscosity of the resin decreases. When reaction becomes fast it starts to dominate the signal and the imaginary impedance maximum increases, as the formation of the network impedes migration of the extrinsic charges. The situation is reversed back to temperature domination towards the end of the reaction. The reaction onset, maximum rate and end points do not coincide with the corresponding points of the impedance versus cure time curves. Consequently following the evolution of maximum impedance cannot provide the means for reaction monitoring under dynamic heating conditions.

Here a different procedure is proposed for the exploitation of impedance data for reaction monitoring. As presented previously the imaginary impedance spectrum has two extremes; a maximum corresponding to charge migration and a minimum at the point where electrode polarisation stops to control the impedance and charge migration becomes the dominant mechanism. Both extremes are shifted during the cure, to lower frequencies as the reaction progresses and to higher frequencies as temperature increases. The minimum of imaginary impedance is shifted outside the experimental spectrum at intermediate to high conversion combined with low and intermediate temperature, thus the available experimental data are limited in isothermal experiments. An observation significant for the monitoring of the

reaction is that the two extremes show similar shifts when temperature changes, whereas the drop of the frequency of the minimum is more sensitive to the reaction progress. This behaviour is manifested clearly in the higher heating rate dynamic curves illustrated in Fig. 9. For example in the 2 ^{o}C/min experiment the maximum shifts by 1.7 decades from 18 to 43 min, while the minimum shifts by 1.8 under the influence of the temperature increase, which is not accompanied by progress of the reaction. In contrast between 79 and 93 min, where the progress of reaction dominates the signal, the maximum shifts by 0.6 and the minimum by 1.4. At high heating rates (1.5, 1.75 and 2 ^{o}C/min) where both the minimum and maximum remain within the measurement frequency range throughout the cure another observation can be made. The minima of the frequencies of the two extremes appearing towards the end of the reaction occur at different times. This is illustrated by the lines which coincide with the minimum of the lower curves (frequency of minimum) in Fig. 9, whereas they intersect with the upper curves (frequency of maximum) at a time later than their minimum.

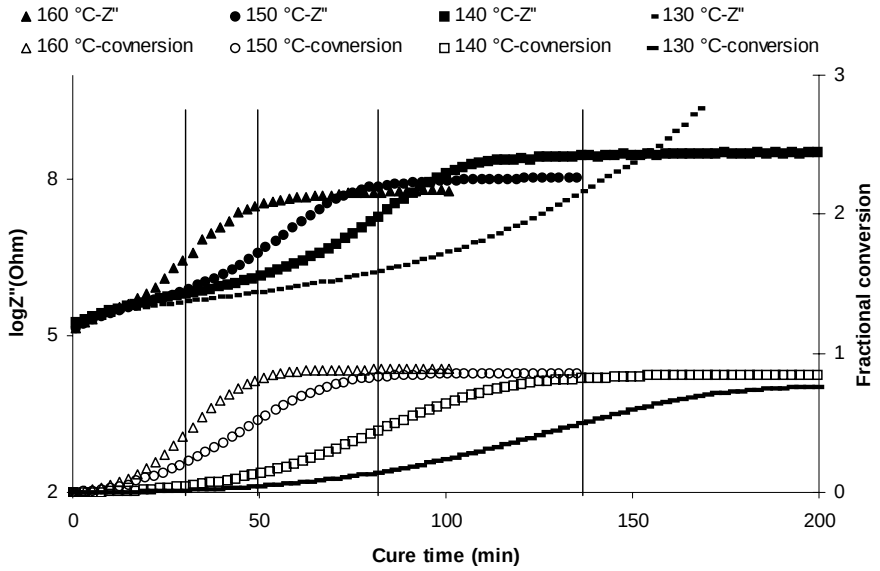

Fig.7 *Imaginary impedance maximum and conversion versus time in isothermal cure*

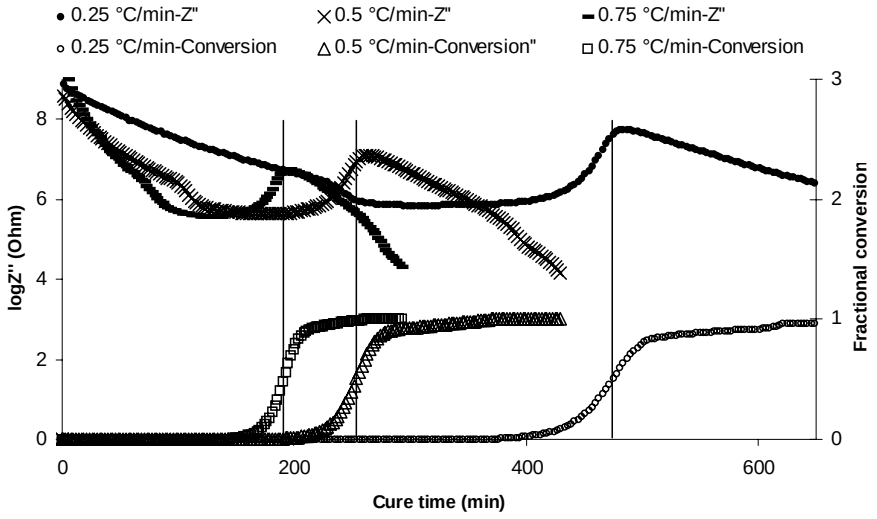

Fig.8 *Imaginary impedance maximum and conversion versus time in dynamic cure of at low heating rates*

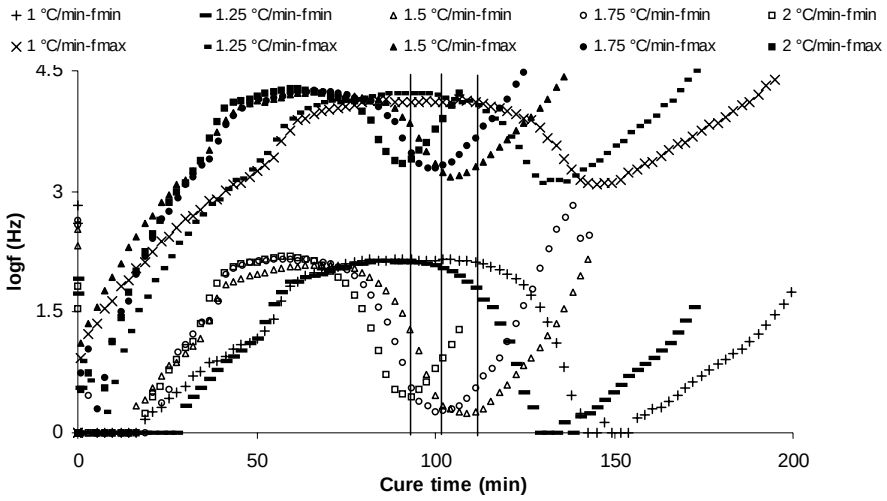

Fig.9 *Frequencies of the impedance spectrum maximum and minimum in dynamic cure of RTM6 resin at high heating rates*

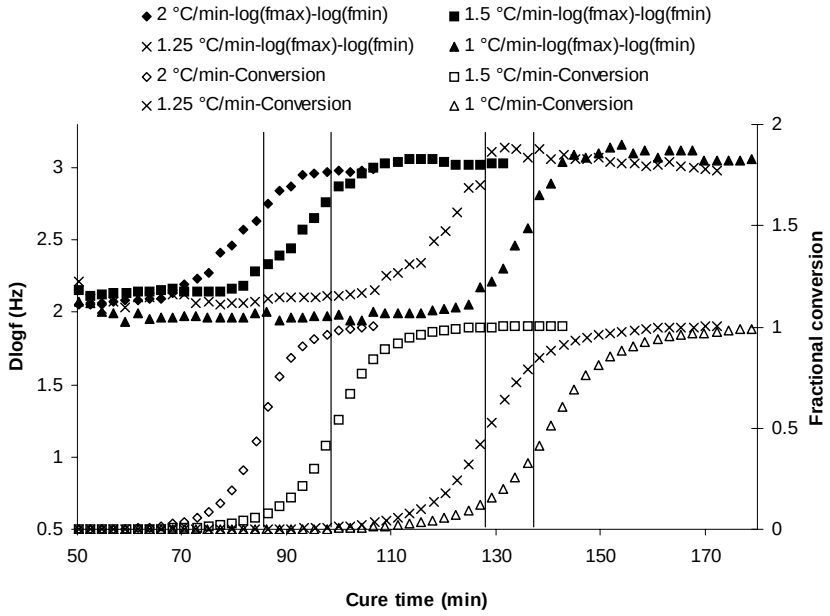

Fig.10 *Impedance spectra maximum and minimum frequencies difference and degree of cure versus cure time in dynamic cure of RTM6*

The different sensitivities of the extremes shift to the progress of the reaction can be used in order to eliminate the problems arising from the combined influence of temperature and degree of cure on the monitoring signals. In Fig. 10 the difference between the frequency of maximum and the frequency of minimum of the imaginary impedance spectrum is compared with the progress of reaction, for the high heating rate dynamic experiments. The frequency difference undergoes a step change. The times of onset, maximum rate and end of the step coincide with the corresponding times of the kinetics curves. When the material does not react the frequency difference remains constant. Thus, the frequency difference shows a strong dependence on the degree of cure, whereas its sensitivity to temperature variation appears low. In order to quantify the correlation, a third degree polynomial was fitted to the data. The equation of the fit is:

$$\alpha = 0.15 D\,log\,f^{3} - 0.38 D\,log\,f^{2} - 0.23 D\,log\,f + 0.81 \quad [7]$$

where α is the fractional conversion and $D\,log\,f$ is the frequency difference. This relation is purely empirical and limited to the specific resin system sensor combination, but it provides the means for a direct estimation of the degree of cure at any temperature from the instantaneous imaginary impedance spectrum.

B. Flow monitoring

Eq. 5 was used to calculate the flow front position from the admittance data. The admittance measured when the sensor is fully covered by resin has been used as Y_{cov}. The real and imaginary part of the length are illustrated together with the visual flow front position measurement in Fig. 11. The average of the error in flow front location and the is 2 cm at 10 kHz and 0.8 cm at 1MHz. It can be observed that data gathered at 1 MHz are very close to the visual flow front measurement. Data obtained at a lower frequency (10 kHz) present some deviation. The imaginary length shows higher value at the frequency where the error in the flow front location estimation is higher, indicating deviation from linearity as described by Eq. 5. Thus, the imaginary length similarly to the non-conductive reinforcement case [16] offers the means for self estimation of the measurement accuracy. Cure monitoring results obtained using the sensing configuration are illustrated in Fig. 12. There, the evolution of normalised impedance at 10 kHz as calculated is shown. It can be observed that the sensing setup has a response equivalent to that of the microelectrodes. Normalised impedance undergoes a step change during the cure and vitrification is manifested as a knee towards the end of the curing.

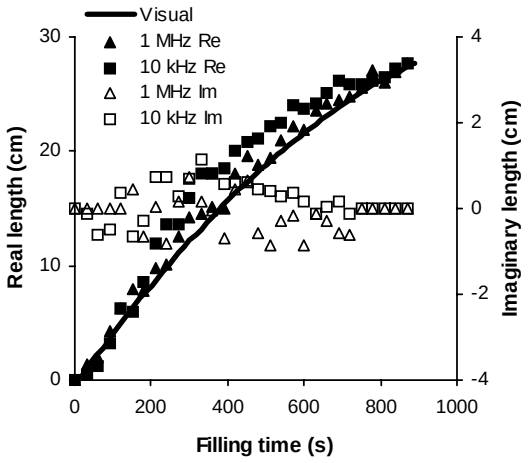

Fig. 11 *Comparison of visual measurement with dielectric flow measurement for filling during resin transfer moulding of an RTM6/carbon composite*

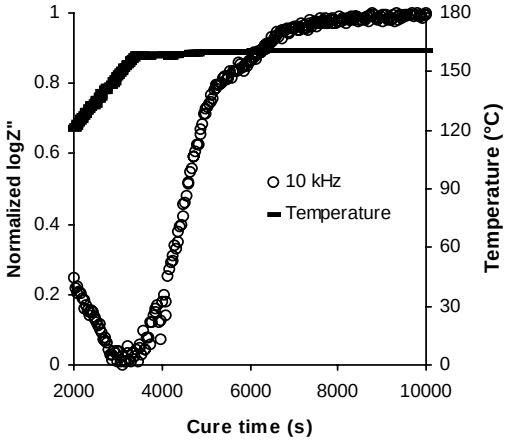

Fig. 12 *Temperature and normalised impedance during cure versus time using the flow monitoring setup in an RTM6/carbon composite moulding*

CONCLUSIONS

Results from the application of impedance spectroscopy to the monitoring of isothermal and dynamic cure of RTM6 epoxy resin and the RTM filling of carbon reinforced compositeshave been presented. The possibility of using impedance spectroscopy for the estimation of the degree of cure in both isothermal and dynamic conditions has been investigated. A purely experimental method based on the different sensitivity of the extremes

of the imaginary impedance spectrum to temperature and conversion has been developed and validated for the specific resin system. A sensing configurations appropriate for flow monitoring during RTM filling of conductive reinforcements was proposed. Equivalent circuit analysis demonstrated the linear dependence of the admittance, measured by the presented sensors, upon the flow front position. Experiments confirmed that the flow front position can be located continuously with a satisfactory accuracy. In addition, the existence of an imaginary component of the measured flow front position can be utilized as self-assessment tool of the measurement performance. The flow sensor also presented the ability to monitor the cure of the resin after the end of the filling stage.

REFERENCES

1. Loos AC and Springer GS, Journal of Composite Materials 17 1983 1352.
2. Tzeng JT and Loos AC, Composites Manufacturing 4 1993 157
3. Gao DM, Trochu F and Gauvin R, Materials and Manufacturing Processes 10 1995 57
4. Hojjati M and Hoa SV, Journal of Composite Materials 29 19951741
5. Tucker CL III, Polymer Composites 17 1996 60
6. Suratno BS, Ye L and Mai YW, Composites Science and Technology 58 1998; 58 191
7. Kranbuehl DE, Kingsley P, Hart S, Hasko G, Dexter B and Loos AC, Polymer Composites 15 1994 299
8. Maistros GM and I. K. Partridge IK, Composites 19B 1998245
9. J. Mijovic J and S. Andjelic S, Polymer 36 1995 3783
10. Woederman DL, Spoerre JK, Flynn KM and Parnas RS, Polymer Composites 18 1997 133
11. Whitney TM and Green RE Jr. Ultrasonics 34 1996 347
12. Shepard DD and Smith KR, Journal of Thermal Analysis 49 1997 95
13. Shepard DD, SAMPE Journal 34 1998 31
14. Barooah P, Berker B and Sun JQ, Journal of Materials Processing and Manufacturing Science 6 1998 169
15. Mathur R, Advani SG, Parnas RS and Fink BK, International SAMPE Technical Conference 29 1997 42
16. Skordos AA, Karkanas PI and Partridge IK, Measurement Science and Technology 11 2000 25
17 Bellucci F, Valentino M, Monneta T, Nicodemo L, Kenny J, Nicolais L and Mijovic J, Journal of Polymer Science Part B: Polymer Physics 32 1994 2519
18. Mijovic J and Yee FCW, Macromolecules 24 1994 7287
19. Mijovic J, Andjelic S, Fitz B, Zurawsky W, Mondragon I, Bellucci F and Nicolais L. Journal of Polymer Science Part B: Polymer Physics 34 1996 379
20. Andjelic S, Mijovic J and Bellucci F, Journal of Polymer Science Part B: Polymer Physics 36 1998 641
21 Skordos AA and Partridge IK Polymer Engineering and Science 41 2001 793